Biosensors and Bioelectronics 193 (2021) 113531

Contents lists available at ScienceDirect

Biosensors and Bioelectronics

journal homepage: www.elsevier.com/locate/bios

Integration of a fiber-based cell culture and biosensing system for monitoring of multiple protein markers secreted from stem cells

Jaehan Ko [a], Jeongwoo Ham [b], Hwajung Lee [b], Kangwon Lee [c,**], Won-Gun Koh [b,*]

[a] Program in Nanoscience and Technology, Graduate School of Convergence Science and Technology, Seoul National University, Seoul, 08826, Republic of Korea
[b] Department of Chemical and Biomolecular Engineering, Yonsei University, Seoul, 03722, Republic of Korea
[c] Department of Applied Bioengineering, Graduate School of Convergence Science and Technology, Seoul National University, Seoul, 08826, Republic of Korea

ARTICLE INFO

Keywords:
Integrated cell culture-biosensor platform
SERS
Electrospun fibers
Cell-secreted biomarker
Stem cell differentiation

ABSTRACT

We propose a new platform that can integrate three-dimensional cell culture scaffold and a surface-enhanced Raman spectroscopy (SERS)-based biosensor by stacking them to form a multilayer system, which would allow monitoring of the protein markers secreted from cultured stem cells without periodic cell and/or media collection. The cell culture scaffold supported the proliferation and osteogenic differentiation of adipose-derived mesenchymal stem cells (ADSCs). The SERS capture substrate detected protein markers in combination with SERS tag made with Au–Ag alloy nanoboxes. Incorporating the different Raman reporters into the SERS tag allowed easy identification of target proteins for multiplex assays. The resultant SERS-based immunoassay could detect the pg/mL levels of protein markers without crosstalk and interference. When one ADSC culture scaffold and multiple SERS capture substrates were integrated and incubated in differentiation culture media, our system was sufficiently sensitive to monitor time-dependent secretion of three different osteogenic protein markers from ADSCs during their osteogenic differentiation. Since the sensor and cell culture scaffold can be manipulated independently, various cell and biomarker combinations are possible to obtain relevant information regarding the actual state of the different types of cells.

1. Introduction

Monitoring secreted protein biomarkers from an in vitro cell culture model is very important for obtaining relevant information regarding the actual state of the cells for fundamental biology research as well as for bioengineering, drug screening, and toxicology (Crevensten et al., 2004; Kamao et al., 2014; Kulkarni and Khanna, 2006; Norström et al., 2006; Pountos et al., 2007; Prabhakaran et al., 2009). In traditional approaches, cells are cultured in Petri dishes or microwell plates, followed by periodic collection of culture media or cells for off-chip analysis. Enzyme-linked immunosorbent assays (ELISAs) are currently the gold standard for such a traditional method, which not only require a large number of cells and/or reagent but also show insufficient sensitivity and selectivity (Aydin, 2015; Crowther, 2001; Sakamoto et al., 2018).

In an effort to develop new methods, platforms that integrate biosensors and cell cultures have been proposed where cells are cultured laterally next to the sensing unit or on the sensing surfaces (Borgmann et al., 2006; Cai et al., 2002; Jung et al., 1999; Modena et al., 2018; Park and Shuler, 2003; Son et al., 2013). Secreted biomarkers are detected optically and electrochemically. For example, nanostructured photonic crystals are utilized for monitoring of the activity of secreted enzymes and the Revzin group proposed several microfabricated systems that could monitor secreted cytokines using fluorescent and electrochemical sensing (Kilian et al., 2007, 2009; Ko et al., 2011; Lee et al., 2009; Liu et al., 2012; Shin et al., 2016; Yan et al., 2009; Zhu et al., 2009). Such an integrated biosensor-cell culture platform possesses the following advantages: 1) allows *in situ* monitoring of a well-defined and small population of cells; 2) does not require cell and media collection; and 3) can miniaturize both biosensor and cell culture using microfabrication techniques. Despite these advantages, there remain several limitations in the current integrated platform. First, cells exist in unnatural environments, such as two-dimensional glass slides, metal electrodes, or nanoporous silicone, which are totally different from real

* Corresponding author. Deparment of Chemical & Biomolecular Engineering, Yonsei University, Seoul 03722, Republic of Korea.
** Corresponding author. Department of Applied Bioengineering, Graduate School of Convergence Science and Technology, Seoul National University, Seoul 08826, Republic of Korea.
E-mail addresses: kangwonlee@snu.ac.kr (K. Lee), wongun@yonsei.ac.kr (W.-G. Koh).

https://doi.org/10.1016/j.bios.2021.113531
Received 23 February 2021; Received in revised form 20 July 2021; Accepted 21 July 2021
Available online 24 July 2021

three-dimensional (3D) environments where cells exist in the human body. Therefore, the response of these cells, including secreted biomarkers during in vitro culture, might be very different to that of cells in native tissue (Abbott, 2003; Levenberg and Langer, 2004). Second, because the sensor and cell culture system are not manufactured and controlled independently, the entire platform becomes unusable if one system does not work properly. Furthermore, few studies have reported the use of an integrated system for the multiplex detection of different biomarkers (Chen et al., 2018; Choi et al., 2020). To the best of our knowledge, the combination of multiplex biosensing with a 3D cell culture system has not previously been reported in an integrated biosensor-cell culture platform.

On the other hands, the identification of the differentiation state of stem cells is a necessary step for the practical application of stem cells in the area of regenerative medicine (Sylvester and Longaker, 2004; Wu and Belmonte, 2016). In addition to the ELISA, three methods, flow cytometry, immunostaining, and polymerase chain reaction (PCR), are mainly used to monitor the differentiation of stem cells (Baghaei et al., 2017; Ren et al., 2020; Sanchez et al., 2016; Siltanen et al., 2016; Sobreiro-Almeida et al., 2017; Ying et al., 2003). These methods detect biomarkers that are secreted during stem cell differentiation and provide information regarding the stage of differentiation as well as the cell types that stem cells have differentiated into. However, these methods interfere with cells by detaching them (flow cytometry, PCR), use harmful treatments (immunostaining, flow cytometry), or destroy them (PCR). To address the above-mentioned limitations, several studies have proposed the use of Raman spectroscopy to monitor stem cell differentiation, where cells are directly irradiated by light without any special treatment (Chiang et al., 2009; Downes et al., 2011; Ghita et al., 2015). The differentiation of stem cells is investigated by detecting the Raman signal originating from the specific biomarker. Although this method is simple, fast, and label-free, there is a possibility of signal overlap between target biomarkers and numerous molecules within cells. Signal interference by auto-fluorescence from the cells may occur when they are excited by light. In addition, incident laser light may have a negative effect on the stem cells.

In this study, we developed a new platform that can integrate the 3D stem cell culture scaffold and biosensor capable of simultaneous detection of multiple differentiation markers. Both the cell culture scaffold and biosensor were prepared from the electrospun fibers, which provide 3D environments to stem cells and excellent sensitivity to biosensors. Surface-enhanced Raman spectroscopy (SERS) was utilized for biosensing, where fibrous sensing scaffolds were coated with silver nanoparticles (AgNPs) and used SERS substrates similarly to the previous studies (C. Chen et al., 2017; Saveleva et al., 2020). The surface of fiber was conjugated with specific antibodies to be used as SERS capture substrates. After confirming that the cell culture scaffold supported the osteogenic differentiation of adipose-derived mesenchymal stem cells (ADSCs) and SERS capture substrate could detect protein markers by combination with SERS tag made with Au–Ag alloy nanoboxes (NBs), both the cell culture scaffold and biosensing substrates were integrated as one platform by stacking each scaffold using a custom-made mold. As a proof-of-concept experiment, we applied the proposed platform to monitor the time-dependent secretion of three different osteogenic differentiation markers (alkaline phosphatase, osteocalcin, and fibronectin). For this, ADSC culture scaffolds were stacked with three different SERS capture substrates, where the biosensing scaffold could be separated independently from the integrated platform and used for SERS-based immunoassay. Since any biosensing scaffold can be removed and added at any time without affecting the cell culture scaffold, the proposed platform was capable of continuously monitoring three differentiation markers for three weeks without interfering with cells.

2. Materials and methods

2.1. Materials

Polycaprolactone (PCL; M_n 80,000), 2, 2, 2-trifluorethanol (TFE), poly(ethylene glycol) diacrylate (PEG-DA) (M_w 575), 2-hydroxy-2-methylpropiophenone (HOMPP), 1X Dulbecco's phosphate-buffered saline (DPBS), phosphate-buffered saline (PBS), tin chloride ($SnCl_2$), palladium chloride ($PdCl_2$), silver nitrate ($AgNO_3$), potassium hydroxide (KOH), ammonium hydroxide (NH_4OH), D-(+)-glucose, HS-PEG 7.5k-COOH, N-(3-dimethylaminopropyl)-N′-ethylcarbodiimide hydrochloride (EDC), N-hydroxysuccinimide (NHS), bovine serum albumin (BSA), hydrogen tetrachloroaurate (III) trihydrate ($HAuCl_4 \cdot 3H_2O$), ascorbic acid (AA), 5,5-dithiobis(2-nitrobenzoic acid) (DTNB), 4-mercaptobenzoic acid (MBA), 4-mercaptophenylboronic acid (MPBA), human serum albumin (HSA), fetal bovine serum (FBS), fibronectin from humans (FN), human alkaline phosphatase (ALP), osteocalcin (OC), dexamethasone, L-ascorbic acid 2-phosphate sesquimagnesium salt hydrate, β-glycerophosphate disodium salt hydrate, alizarin red s (ARS), cetyltrimethylammonium chloride solution (CTAC), 3-(4,5-dimethyl-2-thiazolyl)-2,5-diphenyl-2H-tetrazolium bromide (MTT), RIPA buffer, and the p-nitrophenyl phosphate (pNPP) liquid substrate system were purchased from Sigma-Aldrich (Milwaukee, WI, USA). Anti-FN, -ALP, and –OC were purchased from Abcam (Cambridge, Cambridgeshire, UK). Alexa fluor 488-conjugated IgG (Alexa fluor 488-IgG) and the live/dead viability/cytotoxicity kit were obtained from Invitrogen Corp. (Carlsbad, CA, USA). Photomasks for hydrogel lithography were prepared on transparency sheets using a laser jet printer (LaserWriter 16/600 PS, Apple, Inc., Cupertino, CA, USA).

2.2. Preparation of polycaprolactone nanofiber scaffold

In this study, PCL fibers were used for both the cell culture scaffold and the SERS capture substrates for the SERS assay. Fibers were prepared by the electrospinning technique. The PCL electrospinning solution was prepared as a 10 % w/v solution by dissolving PCL in TFE. After dissolution at 80 °C in a convection oven for 5 h, the solution was transferred to a syringe. A voltage of 8–8.5 kV was applied to the transferred solution in the syringe through the syringe needle (21G). The solution was pushed through the syringe pump at a constant speed of 0.7 mL/h. The electrospun PCL fibers were collected for 1 h by placing the slide glass (18 × 18 mm) covered with aluminum foil on the collection plate and adjusting the height from the needle tip to 20 cm.

2.3. Fabrication of the cell culture scaffold

The hydrogel lithography was applied to the fiber scaffold to incorporate PEG-based hydrogel micropatterns into the fiber as described in our previous studies (Lee and Koh, 2014; Lee et al., 2010). Briefly, the PEG-DA gel precursor solution was prepared by mixing 2 % v/v of HOMPP, a photoinitiator, into a PEG-DA:distilled water (DW) = 1:1 solution. Thereafter, 200 μL of the gel precursor was dropped onto the fiber scaffold, and a photomask of an appropriate pattern was placed on it followed by exposure of 365 nm, 300 mW/cm^2 UV light (EFOS Ultra 100ss Plus, UV spot lamp, Missoga, Ontario, Canada) for 1.6 s. The final cell culture scaffold was obtained by washing out the unreacted gel precursor using DW. The resultant micropatterned fiber scaffold was fixed on a customized mold and sterilized in 70 % v/v ethanol solution for 30 min prior to stem cell culture. After transferring the fiber scaffold to a six-well plate and washing it two-to-three times with 3 mL of DPBS to remove the remaining ethanol, 3 mL of culture media was added for stem cell culturing.

2.4. Fabrication of the SERS capture substrate

The fiber scaffold incorporating PEG hydrogel micropatterns was

obtained using the same experimental procedure as described in the previous section. Here, a patterned scaffold consisting of 16 (4 × 4) fibrous microwells was prepared. The patterned scaffold was coated with silver using a silver mirror reaction (Yun and Koh, 2020). First, the scaffold was treated with oxygen plasma at a 40 W radiofrequency and 0.1 mmHg (Femto Science, Kyunggi, Korea) for 5 min. Afterward, the scaffold was immersed in each of the 3 mM $SnCl_2$ and 3 mM $PdCl_2$ solutions for 20 min. This made the surface of the PCL fiber Pd-seeded, which acts as an active site of nucleation so that the AgNPs can grow easily during coating (Bao et al., 2013). Silver coating was undertaken through the following processes: NH_4OH solution was added to 10 mL of 0.1 M $AgNO_3$ solution containing scaffold until the disappearance of the brown precipitate. Then, 5 mL of 0.8 M KOH solution was added until the solution turned black, and NH_4OH was added again until the color became clear. Finally, when 1 mL of 0.25 M glucose solution and Pd-seeded fiber scaffold were added together, the reduction reaction began and the AgNP-decorated fiber scaffold (Ag-fiber) was obtained.

To immobilize the antibody (anti-FN, -ALP, and –OC) to the obtained Ag-fiber, the Ag-fiber was reacted with 5 mM of HS-PEG7.5k-COOH linker solution for 3 h. Then, Ag-fiber immobilizing linker was reacted with 1 μg/mL antibody solution containing 4 mM EDC and 10 mM NHS solution overnight. Finally, SERS capture substrate was prepared by blocking antibody-immobilized Ag-fiber with 2 % (w/v) BSA solution for 30 min.

2.5. Preparation of SERS tags

SERS tags formed with Au–Ag alloy NBs were synthesized according to the methods of previous studies (Li et al., 2018). First, 450 μL of 25.4 mM $HAuCl_4$ was added to 100 mL of DW in a beaker and stirred at room temperature. Then, 1.7 mL of 6 mM $AgNO_3$ and 300 μL of 0.1 M AA were simultaneously added and reacted for 1 min. The obtained dark blue solution was centrifuged at 600 rcf for 30 min to remove the unreacted material, and the pellet was resuspended in 10 mL of DW. To immobilize the antibodies, 40 μL of 1 mM HS-PEG7.5k-COOH and 200 μL of 1 mM Raman reporters (4-MBA, DTNB, and MPBA) were added to a 2 mL solution of Au–Ag alloy NBs and stirred at room temperature for 6 h. After centrifuging the reacted solution at 600 rcf for 30 min to remove unreacted molecules, antibodies were immobilized onto Au–Ag alloy NBs via the same EDC-NHS reaction followed by the same blocking procedure.

2.6. SERS-based immunoassay

The protein solution was prepared by dissolving the target protein by concentration in PBS. The capture substrates were incubated for 2 h in target protein solutions (FN, ALP) at various concentrations (10 ng/mL, 1 ng/mL, 100 pg/mL, and 10 pg/mL) and washed two-to-three times with DW. Afterward, target-bound capture substrates were immersed in 5 mL of DW containing 200 μL of 3.2 mg/mL SERS tags for 2 h. After washing two-to-three times with DW, Raman signals were detected using Raman spectroscopy (DXR2xi, Thermo Fisher Scientific, Waltham, MA, USA). Raman signals were obtained from each microwell in SERS capture substrates and measurements were made by averaging the values in 16 microwells. Each spot was irradiated with a 785 nm laser for 0.1 s with a power of 1 mW.

2.7. Crosstalk and interference test

The crosstalk test assesses whether the capture substrate reacts with proteins other than the target protein. In this study, an ALP solution of 50 μg/mL was reacted with a SERS capture substrate targeting FN. Then, a FN solution of 10 pg/mL was reacted with a capture scaffold targeting FN. For use as a control group, the capture substrate was also reacted with PBS without proteins. After the corresponding SERS tags were treated on each scaffold, the Raman signals of the three capture substrates were compared. The same experiment was performed using the SERS capture substrate targeting ALP, where 50 μg/mL of FN and 10 pg/mL of ALP were reacted, respectively.

The interference test confirms whether there is a difference in Raman intensity against the target even if other substances are mixed. Overall, 10 pg/mL of the target solution (FN or ALP) in PBS reacted with the capture substrate alone or mixed with other substances, such as HSA and FBS. 10 ng/mL of non-target proteins were dissolved in PBS. For the FBS solution, 10 ng/mL of target protein was dissolved in FBS, and a solution containing all proteins was prepared by dissolving each protein in FBS. After treatment with SERS tags, the Raman signals of each case were compared.

2.8. Culture of ADSCs and their differentiation to osteocytes

ADSCs (Lonza, Basel, Switzerland) were cultured in the cell culture scaffold using control media containing 10 % FBS and 1 % penicillin/streptomycin in Dulbecco's modified Eagle's medium or osteogenic differentiation media (OM) with 100 nM dexamethasone, 100 μM ascorbic acid 2-phosphate, and 10 mM β-glycerophosphate added to the control media. For the control and experimental groups, 3 mL of the control media and OM were added to each microwell. ADSCs (passage 4, 1.0×10^5 cells) were seeded onto the scaffold in each microwell. Cell-seeded scaffolds were incubated at 5 % CO_2, 95 % air, and 37 °C, and the media were changed every two days. The cells were cultured for 21 days.

2.9. Proliferation and viability assay

A fluorescence live/dead assay was used to monitor the cell viability on the cell culture scaffold. This assay used calcein-AM and EthD-1 as fluorophores to stain the living and dead cells, respectively. For this assay, a live/dead solution was prepared by dissolving 2 μM of calcein-AM and 4 μM of EthD-1 in DPBS. After suctioning the culture media, the solution was added to the wells so that the cell culture scaffold was sufficiently immersed. The cell culture scaffold was incubated for 1–1.5 h at 37 °C in the dark. Afterward, the scaffold was washed twice with DPBS and observed with a fluorescent microscope (Carl Zeiss Inc., Thornwood, NY, USA).

A MTT assay was carried out to investigate the cell proliferation on the cell culture scaffold. For this assay, 10 % v/v MTT solution (5 mg/mL) in the DPBS was added to the cell culture scaffold after suctioning the culture media. The scaffold was incubated for 1–1.5 h at 37 °C in the dark, and DMSO was added to the solution to dissolve the formazan produced from MTT by mitochondrial reductase. The absorbance was measured at 540 nm using a microplate reader (Molecular Devices, Sunnyvale, CA, USA).

2.10. ALP activity test and alizarin red s staining

A pNPP assay was used to measure ALP activity, in which ALP hydrolyzes the transparent pNPP and produces yellow p-nitrophenol. The cell culture scaffold was washed with DPBS and 500 μL of RIPA buffer was added to obtain cell lysates, 100 μL of which was mixed with 100 μL of pNPP solution and reacted for 30 min at 37 °C in the dark. The reaction was stopped by addition of 10 μL of 2 M sodium hydroxide solution. The absorbance at 405 nm was measured using a microplate reader.

ADSCs were stained with ARS solution during osteogenic differentiation to monitor the biomineralization. After a certain period of incubation, cultured ADSCs were fixed with 4 % paraformaldehyde for 15 min then stained with 2 % ARS solution for 45 min. After the aspiration of ARS solution and subsequent washing with DW, scaffolds were observed with an optical microscope. Finally, after ARS was extracted with 10 % w/v CTAC in PBS (0.1X, pH 7.4) solution, a 200 μL aliquot was added to a 96-well plate and absorbance was measured at 550 nm

using a microplate reader.

2.11. Multiplex detection of multiple osteogenic biomarkers during the differentiation of ADSCs

First, 2.0×10^5 ADSCs with passage number 4 were seeded into the cell culture scaffold inserted into the customized mold and incubated in a CO_2 incubator for 2 h. Afterward, the SERS capture substrates for three different osteogenic differentiation markers (ALP, FN, and OC) were sequentially inserted into the mold and integrated with cell culture scaffold. Control media were added to the control group, and OM was added to the experimental group. Each medium was changed every two days. The SERS capture substrates were separated every two days from the mold and reacted with corresponding SERS tag. The Raman signal was measured at seven time points (Day 1, 5, 9, 13, 15, 17, and 21).

3. Results and discussion

The platform used in this study was composed of multiple scaffolds formed from a hydrogel-incorporated fiber matrix. One scaffold was used for the culture of stem cells and the other for SERS capture substrate for the detection of specific targets. Each scaffold was combined so that differentiation protein markers secreted from cultured stem cells could be detected via SERS-based immunoassays (Fig. 1). The cell culture scaffold was placed at the bottom for the differentiation of stem cells, while SERS capture substrates were placed above the cell culture scaffold, which can detect substances secreted by stem cells. By stacking multiple capture substrates, it is possible to detect multiple markers independently and have higher spatial efficiency than arranging scaffolds sideways. At a set time, a specific capture substrate could be separated from the scaffold assembly and used for quantitative SERS-based immunosensing.

3.1. Fabrication of fiber-based scaffolds for ADSC culture and SERS-based biosensing

Both the cell culture scaffold and SERS capture substrate were prepared by combining the electrospinning and hydrogel patterning processes. Electrospinning produced ultrathin PCL fibers with a diameter of 1051 ± 134.5 nm. The average pore size was approximately 6.4 μm, which was sufficiently large for target markers secreted from cells to diffuse rapidly from the cell culture scaffold to the SERS capture substrate. To incorporate hydrogel patterns into electrospun fibers, a photomask containing arrays of square patterns (2 × 2 mm or 5 × 5 mm) was used (Fig. 2a). According to the photomask design, only the precursor solution under the transparent region underwent UV-induced photocrosslinking and became an insoluble hydrogel pattern, creating an array of fiber-based microwells separated by hydrogel walls, as shown in optical images in Fig. 2b and c. Incorporation of the hydrogel pattern made the handling of the μm-thick fibrous scaffold easy, otherwise PCL-based fibers would fold and aggregate in aqueous environment due to their hydrophobicity. Furthermore, hydrogel patterning process did not cause any significant change on the fiber morphology (SEM images in Fig. 2b).

For the cell culture scaffold, four microwells (size of each microwell: 5 × 5 mm) were prepared to secure as wide a culture zone as possible while preventing the fiber scaffold from sagging (Fig. 2b). On the other hands, 4 × 4 arrays of microwells (size of each microwell: 2 × 2 mm) were fabricated for SERS capture substrate (Fig. 3c). Each microwell in the SERS capture substrate played a role as a single sensor and, subsequently, increased the reliability of the measurements by obtaining multiple Raman intensities from different microwells. The SERS capture substrate underwent silver mirror reaction to grow the AgNPs on the fiber surface via the reduction of silver ions using glucose as shown in SEM image of Fig. 2c. The formation of AgNPs was confirmed with SEM-EDS analysis (Fig. 2d). A large amount of silver was observed in fibers that underwent silver mirror reactions, while no silver was detected in the SEM-EDS images of bare fibers (Fig. S1 in Supplementary Materials).

The fluorescence method was used to confirm the covalent protein immobilization on the AgNP-decorated fiber surface via the bifunctional linker. Alexa fluor 488-IgG was incubated with capture substrates with and without bifunctional linker to visualize protein immobilization. As shown in Fig. S2 in Supplementary Materials, strong green fluorescence was only observed from the scaffold modified with the bifunctional linker, while a very weak fluorescence signal was observed from the scaffold without the bifunctional linker. This result demonstrated that the bifunctional linker was successfully attached to the AgNP-decorated PCL fibers and could covalently immobilized the proteins, while few proteins could be physically adsorbed onto the AgNP-decorated PCL fibers.

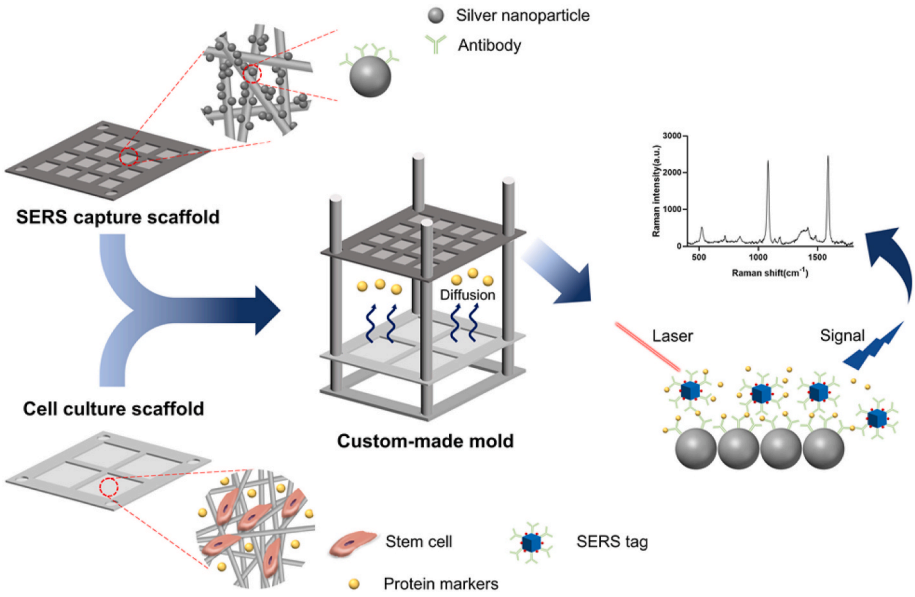

Fig. 1. Schematic illustration of integrating 3D cell culture scaffold and SERS-based biosensor for the detection of protein markers secreted from stem cells.

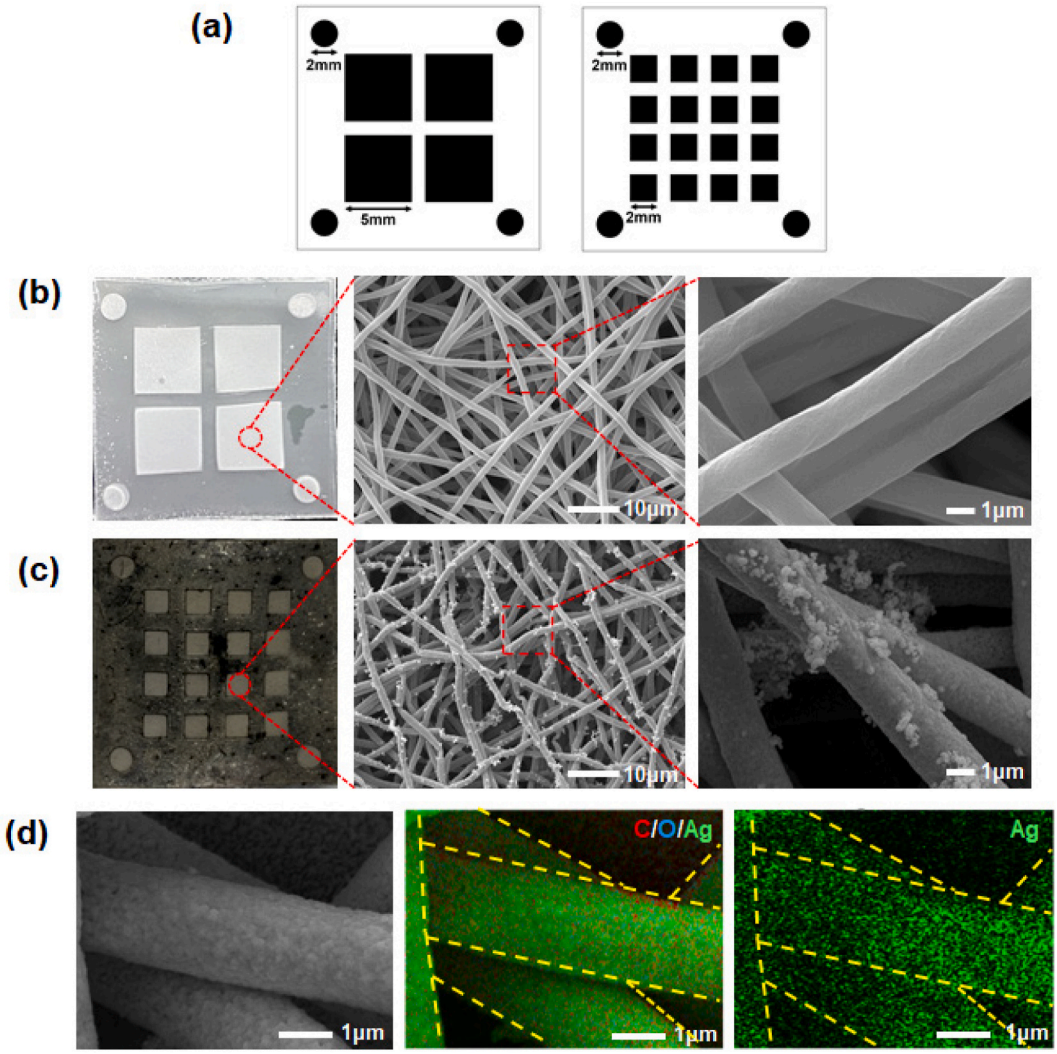

Fig. 2. Preparation of fiber scaffold incorporating hydrogel micropatterns for 3D cell culture and SERS-based biosensing. (a) Photomask designs for 3D cell culture scaffold (left) and SERS capture substrate (right). Optical and SEM images of (b) 3D cell culture scaffold and (c) SERS capture substrate. (d) SEM-EDS mapping images of SERS capture substrate.

3.2. ADSC culture

Before confirming the osteogenic differentiation of ADSCs within the cell culture scaffold, we first investigated the cytocompatibility of the cell culture scaffold by investigating the proliferation and viability of ADSCs (Fig. S3 in Supplementary Material). Osteogenic differentiation media (OM) was used for the differentiation of ADSCs into bone, while normal culture medium was used for the control group (Y. Chen et al., 2017; Langenbach and Handschel, 2013). According to the MTT assay shown in Fig. S3a, ADSCs in the cell culture scaffold remained viable and proliferated in both cell culture media. The viability of ADSCs cultured in OM was also confirmed with a fluorescence live/dead assay, where living and dead cells emitted green and red fluorescence, respectively. As green fluorescence was observed in most cells, it could be confirmed that the cells were alive in the scaffold. It was also confirmed that cells could proliferate on the scaffold through the increase in the number of living cells with time (Fig. S3b).

For the investigation of the osteogenic differentiation of ADSCs, the activity of ALP, an early stage marker for osteoblastic differentiation (Miron and Zhang, 2012), was analyzed for 21 days using a pNPP assay (Fig. 3a). There was a dramatic increase in ALP activity between one and two weeks only from ADSCs cultured in OM. The osteogenic differentiation of ADSCs was further examined with ARS, which is a dye that stains calcium deposition and allows the observation of calcium secreted from the osteocytes. Optical images revealed that ADSCs cultured in OM were more strongly stained than those in control media after 14 days of culture, and the difference became more significant after 21 days (Fig. 3b). For the quantitative evaluation of ARS staining, the absorbance of extract solution was measured. Although there was no significant difference in absorbance until the seventh day, a significant difference was observed after 14 days of culture, and this difference became more evident after 21 days, as shown in Fig. 3c, which was in accordance with the optical image results. These results confirmed that the cell culture scaffold and OM supported the proliferation and osteogenic differentiation of ADSCs.

3.3. SERS-based immunoassay

Both gold nanoparticles (AuNPs) and AgNPs are often used for SERS tags (Li et al., 2019; Plou et al., 2020; Qian et al., 2008; Sloan-Dennison et al., 2019). AuNPs are more biocompatible and stable than AgNPs. However, spherical AuNPs have a relatively small SERS signal amplification compared to those with an asymmetric nanostructure. The asymmetrical shapes is known to generate more amplified Raman signal than symmetric spherical shape due to the shape effect that the pointed parts of the metal magnifies the resonance (Boyack and Le Ru, 2009;

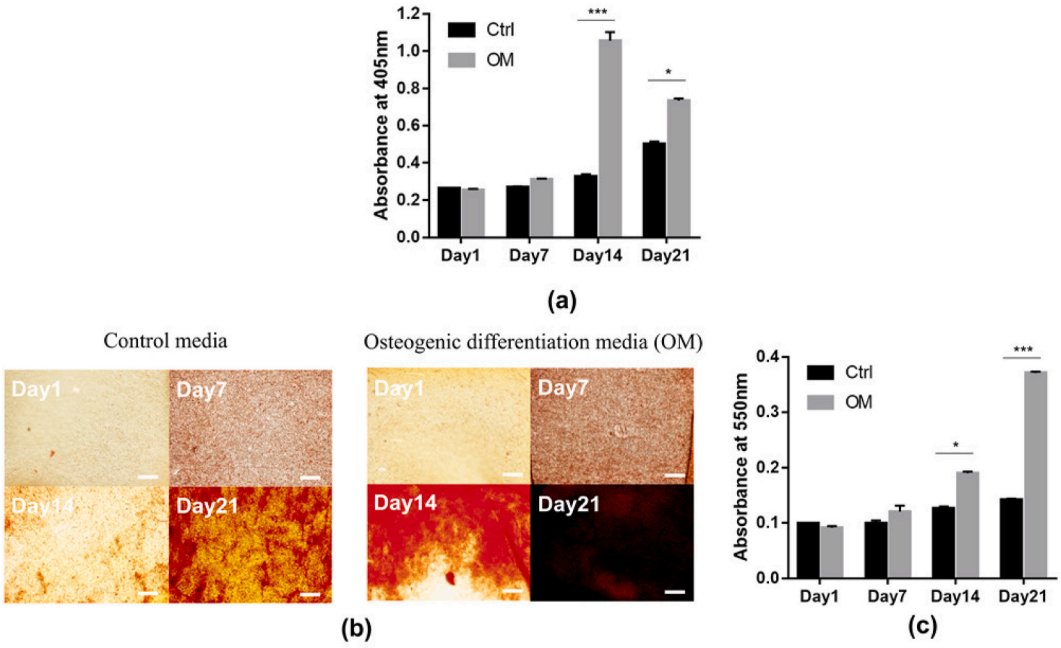

Fig. 3. Osteogenic differentiation of ADSCs cultured on the cell culture scaffold. (a) Graph of ALP activity at different time points. (b) Images of ADSC stained with ARS at each time point. Calcium deposition is stained red. Scale bar = 400 μm. (c) Quantitative analysis of ARS staining where absorbance of the solution extracted from ARS-stained cells was plotted at each time point. Data are represented as the mean ± SEM (n = 4). Significance was calculated by one-way ANOVA with Tukey's post hoc test, *p ≤ 0.05, **p ≤ 0.01, ***p ≤ 0.001. (For interpretation of the references to color in this figure legend, the reader is referred to the Web version of this article.)

Mulvihill et al., 2010). Furthermore, AuNPs have a relatively small signal amplification due to weaker resonance than AgNPs (Kelly et al., 2003). In this study, to overcome the problems arising from spherical AuNPs, we used Au–Ag alloy NBs as the main nanomaterials of the SERS tags (Fig. S4 in Supplementary Materials). TEM imaging confirmed that the 80–100 nm NBs were successfully synthesized (Fig. S4a). Since this box-shaped gold nanostructure has more edges than a spherical shape, many 'hot spots' are formed and subsequently provide a much stronger Raman signal (Mulvihill et al., 2010). By using Au–Ag alloy NBs as SERS tags through alloying gold with silver, the Raman signal was amplified more than 10 times compared to using gold spherical nanoparticles as SERS tags (Li et al., 2018). Moreover, even if they were stored for a long time, Au–Ag alloy NBs would not aggregate. The final SERS tag was completed by immobilizing antibodies and Raman reporters to the synthesized NB. Three different Raman reporters (DTNB, MPBA and MBA) were used in this study to facilitate the detection of multiple markers. For DTNB, the disulfide bond was broken and bound to NB via metal (Au or Ag)-sulfur bonds (Biebuyck and Whitesides, 1993; Darder et al., 1999). MPBA and MBA were bound to NB through the thiol groups present in each molecule (Castner et al., 1996). Antibodies were covalently immobilized onto Au–Ag alloy (NB) using HS-PEG7.5k-COOH, which was similar to the immobilization of antibodies onto SERS capture substrate described in the previous section 2.4. After preparation of the SERS tag conjugating antibodies and Raman reporters, we first verified the existence of the SERS signal from each Raman reporter in the SERS tag. The Raman spectra in Fig. S4b show a peak at 1326 and 1560 cm^{-1}, which are signature peaks of DTNB, as well as at 1070 and 1575 cm^{-1}, which are signature peaks of MPBA and MBA, respectively. These results demonstrated that SERS tags immobilizing different Raman reporters were successfully prepared and distinguishable Raman peaks were detected from each SERS tag. Although the MPBA and MBA signature peaks appeared similar, the two Raman reporters were distinguished by a difference of peak at 521 cm^{-1}.

Next, we performed immunoassay detection of two different proteins, such as FN and ALP, using prepared SERS capture substrate and SERS tag. For the detection of target proteins, antibodies for FN and ALP were immobilized onto capture substrate and SERS tag, while DTNB and MBA were incorporated for the identification of ALP and FN, respectively. Various concentrations (1 mg/mL, 10 ng/mL, 1 ng/mL, 100 pg/mL, and 10 pg/mL) of the target proteins in PBS reacted to capture substrate so that target proteins were bound to their corresponding antibodies on the fibers. Although Raman signals were observed from the capture substrate without the SERS tag after the reaction with ALP and FN, it was difficult to distinguish the two types of proteins by only the Raman peak due to similarity of the Raman spectra for both targets (Fig. 4a). However, if SERS tags incorporating different Raman reporters are processed, both target proteins can be easily distinguished by signature peaks of DTNB (ALP) and MBA (FN) as shown in Fig. 4b. Fig. 4b also indicates that signature peaks of DTNB and MBA gradually increased as the concentration of FN and ALP increased. Based on the Raman spectra, SERS intensity peaks at 1320-1330 cm^{-1} for DTNB and 1070 cm^{-1} for MBA were plotted according to the concentration of ALP and FN, as shown in Fig. 4c. Both assays sufficiently detected target proteins up to 10 pg/mL. Considering that the concentration of proteins secreted from cultured cells ranges from ng/mL to μg/mL per week, our proposed SERS-based immunoassay platform is sufficiently sensitive to detect various protein markers secreted from the cells (Eriksen et al., 1982; Gundberg et al., 1985; Walter and Schütt, 1974).

Moreover, the possible crosstalk between the two target proteins was investigated, as shown in Fig. 5a. In spite of the presence of high concentrations of non-target protein, both immunoassays showed excellent responses to the low concentration of target proteins and very low responses to non-target proteins. For example, in the ALP sensing system, the Raman signal for 10 pg/mL of ALP was much stronger than that of FN at a concentration of 50 μg/mL. The Raman signal of FN 50 μg/mL was similar to that of the blank solution. The same trend was observed for the FN sensing system. These results indicate that the proposed SERS-based immunoassay system have little crosstalk between target and non-target protein. One of the main problems in detecting specific proteins in cell culture media is the interference caused by various proteins that exist in serum or secreted from cultured cells. These possible interferences by other proteins were studied by comparing the Raman

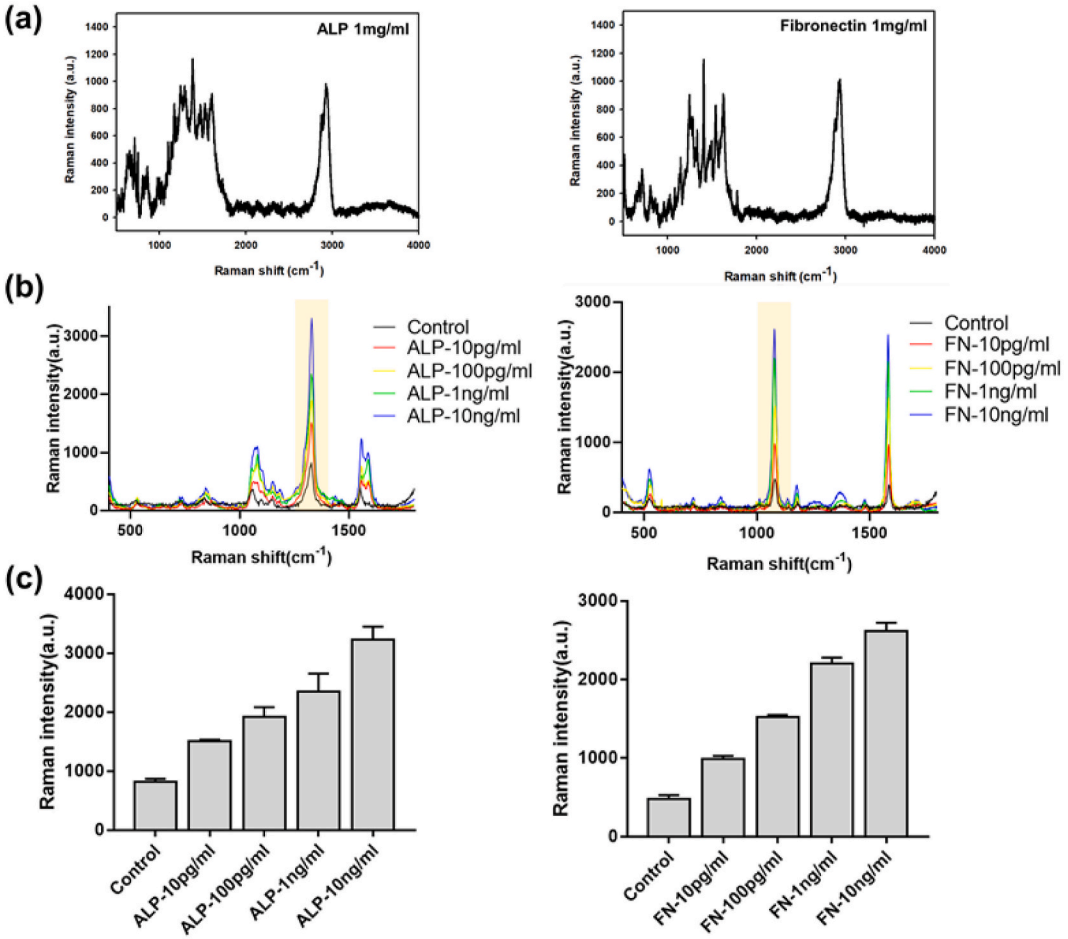

Fig. 4. Detection of protein markers (ALP and FN) using SERS capture substrate. (a) SERS spectra obtained after binding of target proteins (1 mg/mL) on the antibody-immobilized capture substrate without SERS tag (Left: Raman spectrum for ALP, Right: Raman spectrum for FN). (b) SERS spectra acquired from a sandwich immunoassay with SERS tag using different concentration of ALP (left) and FN (right). (c) Intensity of signature peak as a function of target concentration.

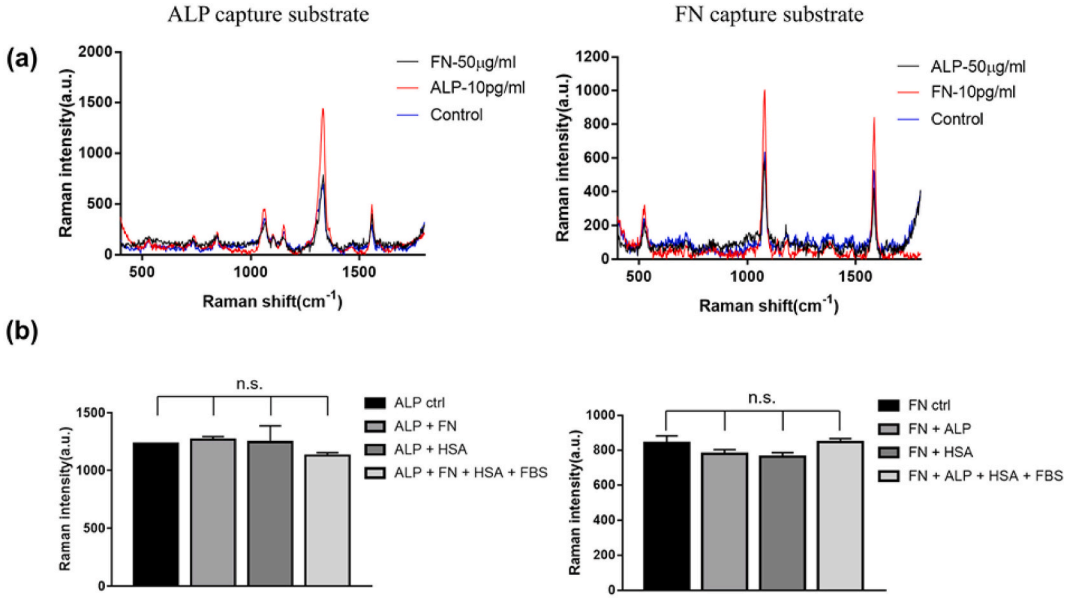

Fig. 5. Crosstalk and interference test of SERS-based immunoassay using prepared capture substrate and SERS tag. (a) Investigation of crosstalk. SERS spectra were obtained after reaction with sample solution containing high concentration of non-target protein and low concentration of target protein. (b) Interference test showing Raman intensities measured from ALP (left) and FN (right) which were included in different mixture solutions.

signal between the target-only sample and the mixture of target and other proteins. Regardless of the type or number of proteins mixed together, a similar Raman signal was detected with no significant difference from the sample containing only target protein for both ALP and FN, as shown in Fig. 5b. These results confirmed the excellent selectivity of our immunoassay system with very low interference from non-target proteins.

3.4. Detection of multiple differentiation makers during osteogenesis of ADSC

After confirming that cell culture scaffolds and SERS capture substrates were successfully used for ADSC culture and immunoassay, one cell culture scaffold and three SERS capture substrates were combined into a custom-made mold to monitor the differentiation of stem cells continuously. For this, differentiation markers secreted from ADSCs in the cell culture scaffold were detected via a SERS-based immunoassay by using SERS capture substrates. Among the various protein markers secreted by ADSCs during osteogenesis, ALP, OC, and FN were selected in this study since they are well-known biomarkers expressed during osteogenic differentiation. For example, ALP can be identified as an early-stage marker secreted from pre-osteoblasts to mature osteoblasts, and OC secreted only from osteoblasts can be identified as a middle stage marker. FN, which is secreted by both osteoblasts and osteocytes, can be identified as a late stage marker (Fig. 6a) (Miron and Zhang, 2012; Rutkovskiy et al., 2016; Zhang et al., 2018). For the simultaneous detection of these three markers, three different SERS capture substrates immobilizing antibodies for ALP, OC, and FN were stacked over the cell culture scaffold as shown in Fig. 6b. For easy identification of target proteins, SERS tags immobilizing different Raman reporters were used for ALP, OC, and FN (ALP: DTNB, OC: MPBA, FN: MBA).

According to the Raman signal obtained from the immunoassays (Fig. 6c and Fig. S5~S7 in Supplementary Materials), ADSCs cultured in OM secreted more differentiation markers than those in the control media. Analyzing the results in OM according to the culture period showed that all three markers were rarely secreted during the first week in the osteoprogenitor state. Most ALP was secreted between the first and second week of culture, but no ALP was detected after 15 days. OC was mostly secreted after two weeks, but it was no longer secreted after 17 days. FN was continuously secreted throughout the differentiation periods commencing after one week. These secretion behaviors of ADSCs are consistent with the results of previous studies. In contrast, in the control group, ALP and OC were only slightly secreted during the first and second week. FN was intermittently secreted without any particular tendency. In particular, FN was secreted extensively on the fifth day. Considering that FN is an important protein for the formation of the ECM, it is inferred that its secretion in the early period of culture was due to the production of the ECM from the non-differentiated cells. These results suggest that the platform we designed works well as a cell culture scaffold for ADSC differentiation and as a sensor for the simultaneous detection of various differentiation markers. It was also expected that the proposed platform could be sufficiently used not only for monitoring the differentiation of various stem cells but also for detecting various metabolites from cultured cells. Although we demonstrated the use of one SERS capture scaffold for the detection of one target, one capture scaffold would be designed to immobilize multiple antibodies in different regions of substrate so that multiple markers can be detected in one SERS capture scaffold.

4. Conclusion

We developed a multi-layered scaffold platform capable of 3D culture of ADSCs and simultaneous detection of multiple differentiation markers. Both cell culture and sensing scaffolds were prepared by electrospun nanofibers incorporating hydrogel patterns. In particular, sensing scaffolds were coated with AgNPs and conjugated with specific antibodies, which were used as SERS capture substrates for immunoassays. Each scaffold was integrated as one platform by stacking them using a custom-made mold. The cell culture scaffold successfully supported the proliferation and differentiation of ADSCs in OM, while SERS capture substrate detected various protein markers in combination with SERS tag made with Au–Ag alloy NBs. When one ADSC culture scaffold and multiple SERS capture substrates for target markers were integrated and incubated in OM, time-dependent secretion of three different

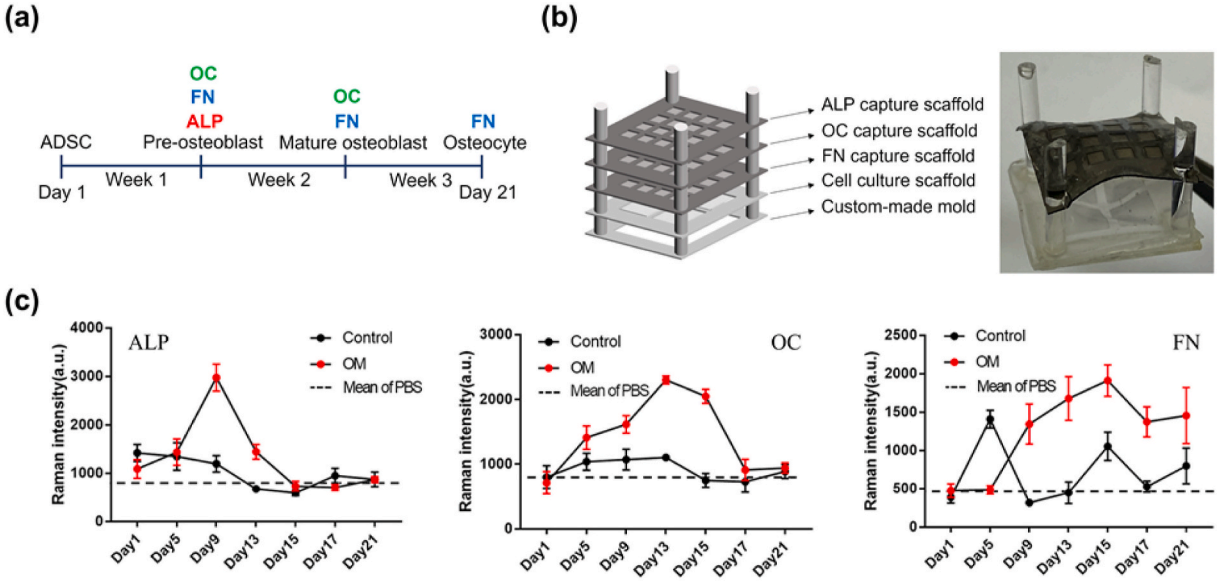

Fig. 6. Monitoring the osteogenic differentiation of ADSCs using multilayer scaffold system integrating 3D cell culture scaffold and SERS capture substrate. (a) Osteogenic differentiation process and expression profile of three different osteogenic protein markers used in this study. (b) Integration of cell culture scaffold and three different SERS capture substrates via a custom-made mold. (c) Raman intensity changes by ALP, OC and FN secreted from ADSCs at different culture time. The control and OM represent the results obtained from ADSCS cultured in control media and osteogenic differentiation media, respectively. Raman intensities in each graph were obtained from different Raman reporters for ALP, OC, and FN (ALP: DTNB, OC: MPBA, FN: MBA). The dotted line represents the average value of Raman intensity obtained from SERS-based immunoassay using PBS solution without any protein marker. All data are represented as the mean ± SEM (n = 5).

osteogenic differentiation markers (ALP, OC, and FN) was successfully monitored for three weeks. We expected that the proposed platform would overcome the limitations of the existing methods of identifying the differentiation of stem cells as it does not require any harmful treatment of cells and can carry out the assay continuously with a single platform. Since the multiple sensing scaffold can be stacked vertically, many types of biomarkers are detected simultaneously, and it is more spatially efficient than the horizontal arrangement. Furthermore, this system is labor-efficient since it does not require cell and media collection.

CRediT authorship contribution statement

Jaehan Ko: Methodology, Validation, Visualization, Writing – original draft. **Jeongwoo Ham:** Methodology, Validation, Visualization. **Hwajung Lee:** Methodology, Validation. **Kangwon Lee:** Conceptualization, Supervision, Writing – review & editing. **Won-Gun Koh:** Conceptualization, Supervision, Writing – review & editing.

Declaration of competing interest

The authors declare that they have no known competing financial interests or personal relationships that could have appeared to influence the work reported in this paper.

Acknowledgements

This research was supported by the National Research Foundation of Korea (NRF) funded by the Ministry of Science and ICT (MSIT) of Korea government (2017M3D1A1039289, 2017M3A7B4041798 and 2017M3A7B4049850).

Appendix A. Supplementary data

Supplementary data to this article can be found online at https://doi.org/10.1016/j.bios.2021.113531.

References

Abbott, A., 2003. Biology's New Dimension, Secondary. Nature Publishing Group.
Aydin, S., 2015. Peptides 72, 4–15.
Baghaei, K., Hashemi, S.M., Tokhanbigli, S., Rad, A.A., Assadzadeh-Aghdaei, H., Sharifian, A., Zali, M.R., 2017. Gastroenterol. Hepatol. Bed. Bench. 10, 208.
Bao, Y., Lai, C., Zhu, Z., Fong, H., Jiang, C., 2013. RSC Adv. 3, 8998–9004.
Biebuyck, H.A., Whitesides, G.M., 1993. Langmuir 9, 1766–1770.
Borgmann, S., Radtke, I., Erichsen, T., Blöchl, A., Heumann, R., Schuhmann, W., 2006. Chembiochem 7, 662–668.
Boyack, R., Le Ru, E.C., 2009. Phys. Chem. Chem. Phys. 11, 7398–7405.
Cai, X., Klauke, N., Glidle, A., Cobbold, P., Smith, G.L., Cooper, J.M., 2002. Anal. Chem. 74, 908–914.
Castner, D.G., Hinds, K., Grainger, D.W., 1996. Langmuir 12, 5083–5086.
Chen, C., Tang, Y., Vlahovic, B., Yan, F., 2017. Nanoscale Res. Lett 12, 1–15.
Chen, H., Chen, C., Bai, S., Gao, Y., Metcalfe, G., Cheng, W., Zhu, Y., 2018. Nanoscale 10, 20196–20206.
Chen, Y., Li, J., Kawazoe, N., Chen, G., 2017. J. Mater. Chem. B 5, 6801–6810.
Chiang, H.K., Peng, F.Y., Hung, S.C., Feng, Y.C., 2009. J. Raman Spectrosc. 40, 546–549.
Choi, N., Dang, H., Das, A., Sim, M.S., Chung, I.Y., Choo, J., 2020. Biosens. Bioelectron. 164, 112326.
Crevensten, G., Walsh, A.J., Ananthakrishnan, D., Page, P., Wahba, G.M., Lotz, J.C., Berven, S., 2004. Ann. Biomed. Eng. 32, 430–434.
Crowther, J.R., 2001. Immunochemical Techniques, the ELISA Guidebook. Springer, pp. 395–405.
Darder, M., Takada, K., Pariente, F., Lorenzo, E., Abruña, H.D., 1999. Anal. Chem. 71, 5530–5537.
Downes, A., Mouras, R., Bagnaninchi, P., Elfick, A., 2011. J. Raman Spectrosc. 42, 1864–1870.
Eriksen, H.O., Clemmensen, I., Hansen, M.S., Ibsen, K.K., 1982. Scand. J. Clin. Lab. Invest. 42, 291–295.
Ghita, A., Pascut, F.C., Sottile, V., Denning, C., Notingher, I., 2015. EPJ Tech. Instrum. 2, 1–14.
Gundberg, C.M., Markowitz, M.E., Mizruchi, M., Rosen, J.F., 1985. J. Clin. Endocrinol. Metab. 60, 736–739.
Jung, S.-K., Gorski, W., Aspinwall, C.A., Kauri, L.M., Kennedy, R.T., 1999. Anal. Chem. 71, 3642–3649.
Kamao, H., Mandai, M., Okamoto, S., Sakai, N., Suga, A., Sugita, S., Kiryu, J., Takahashi, M., 2014. Stem Cell Rep 2, 205–218.
Kelly, K.L., Coronado, E., Zhao, L.L., Schatz, G.C., 2003. J. Phys. Chem. B 107, 668–677.
Kilian, K.A., Böcking, T., Gaus, K., Gal, M., Gooding, J.J., 2007. Biomaterials 28, 3055–3062.
Kilian, K.A., Lai, L.M., Magenau, A., Cartland, S., Böcking, T., Di Girolamo, N., Gal, M., Gaus, K., Gooding, J.J., 2009. Nano Lett. 9, 2021–2025.
Ko, P.J., Ishikawa, R., Takamura, T., Morimoto, Y., Cho, B., Sohn, H., Sandhu, A., 2011. Nanosci. Nanotechnol. Lett. 3, 612–616.
Kulkarni, J., Khanna, A., 2006. Toxicol. Vitro 20, 1014–1022.
Langenbach, F., Handschel, J., 2013. Stem Cell Res. Ther. 4, 1–7.
Lee, H.J., Koh, W.-G., 2014. ACS Appl. Mater. Interfaces 6, 9338–9348.
Lee, H.J., Nam, S.H., Son, K.J., Koh, W.-G., 2010. Sensor. Actuator. B Chem. 148, 504–510.
Lee, J.Y., Shah, S.S., Yan, J., Howland, M.C., Parikh, A.N., Pan, T., Revzin, A., 2009. Langmuir 25, 3880–3886.
Levenberg, S., Langer, R., 2004. Curr. Top. Dev. Biol. 61, 113–134.
Li, J., Wang, J., Grewal, Y.S., Howard, C.B., Raftery, L.J., Mahler, S., Wang, Y., Trau, M., 2018. Anal. Chem. 90, 10377–10384.
Li, M., Wu, J., Ma, M., Feng, Z., Mi, Z., Rong, P., Liu, D., 2019. Nanotheranostics 3, 113.
Liu, Y., Kwa, T., Revzin, A., 2012. Biomaterials 33, 7347–7355.
Miron, R.J., Zhang, Y.F., 2012. J. Dent. Res. 91, 736–744.
Modena, M.M., Chawla, K., Misun, P.M., Hierlemann, A., 2018. ACS Chem. Biol. 13, 1767–1784.
Mulvihill, M.J., Ling, X.Y., Henzie, J., Yang, P., 2010. J. Am. Chem. Soc. 132, 268–274.
Norström, A., ÅKesson, K., Hardarson, T., Hamberger, L., BjöRquist, P., Sartipy, P., 2006. Exp. Biol. Med. 231, 1753–1762.
Park, T.H., Shuler, M.L., 2003. Biotechnol. Prog. 19, 243–253.
Plou, J., García, I., Charconnet, M., Astobiza, I., García-Astrain, C., Matricardi, C., Mihi, A., Carracedo, A., Liz-Marzán, L.M., 2020. Adv. Funct. Mater. 30, 1910335.
Pountos, I., Corscadden, D., Emery, P., Giannoudis, P.V., 2007. Injury 38, S23–S33.
Prabhakaran, M.P., Venugopal, J.R., Ramakrishna, S., 2009. Biomaterials 30, 4996–5003.
Qian, X., Peng, X.H., Ansari, D.O., Yin-Goen, Q., Chen, G.Z., Shin, D.M., Yang, L., Young, A.N., Wang, M.D., Nie, S., 2008. Nat. Biotechnol. 26, 83–90.
Ren, N., Liang, N., Yu, X., Wang, A., Xie, J., Sun, C., 2020. Nanotechnology 31, 145101.
Rutkovskiy, A., Stensløkken, K.O., Vaage, I.J., 2016. Med. Sci. Monit. Basic. Res. 22, 95–106.
Sakamoto, S., Putalun, W., Vimolmangkang, S., Phoolcharoen, W., Shoyama, Y., Tanaka, H., Morimoto, S., 2018. J. Nat. Med. 72, 32–42.
Sanchez, C.G., Teixeira, F.K., Czech, B., Preall, J.B., Zamparini, A.L., Seifert, J.R., Malone, C.D., Hannon, G.J., Lehmann, R., 2016. Cell stem cell 18, 276–290.
Saveleva, M., Prikhozhdenko, E., Gorin, D., Skirtach, A.G., Yashchenok, A., Parakhonskiy, B., 2020. Front. Chem. 7, 888.
Shin, S.R., Zhang, Y.S., Kim, D.-J., Manbohi, A., Avci, H., Silvestri, A., Aleman, J., Hu, N., Kilic, T., Keung, W., 2016. Anal. Chem. 88, 10019–10027.
Siltanen, C., Yaghoobi, M., Haque, A., You, J., Lowen, J., Soleimani, M., Revzin, A., 2016. Acta Biomater. 34, 125–132.
Sloan-Dennison, S., Bevins, M.R., Scarpitti, B.T., Sauvé, V.K., Schultz, Z.D., 2019. Analyst 144, 5538–5546.
Sobreiro-Almeida, R., Tamaño-Machiavello, M.N., Carvalho, E., Cordon, L., Doria, S., Senent, L., Correia, D., Ribeiro, C., Lanceros-Méndez, S., Sabater i Serra, R., 2017. Int. J. Mol. Sci. 18, 2391.
Son, K.J., Shin, D.-S., Kwa, T., Gao, Y., Revzin, A., 2013. Anal. Chem. 85, 11893–11901.
Sylvester, K.G., Longaker, M.T., 2004. Arch. Surg. 139, 93–99.
Walter, K., Schütt, C., 1974. Alkaline phosphatase in serum: continuous assay. In: Bergmeyer, H.U. (Ed.), Methods of Enzymatic Analysis, second ed. Academic Press, pp. 860–864.
Wu, J., Belmonte, J.C.I., 2016. Cell 165, 1572–1585.
Yan, J., Sun, Y., Zhu, H., Marcu, L., Revzin, A., 2009. Biosens. Bioelectron. 24, 2604–2610.
Ying, Q.-L., Nichols, J., Chambers, I., Smith, A., 2003. Cell 115, 281–292.
Yun, B.J., Koh, W.-G., 2020. J. Ind. Eng. Chem. 82, 341–348.
Zhang, D., Zhou, C., Wang, Q., Cai, L., Du, W., Li, X., Zhou, X., Xie, J., 2018. Cell. Physiol. Biochem. 51, 1013–1026.
Zhu, H., Stybayeva, G., Silangcruz, J., Yan, J., Ramanculov, E., Dandekar, S., George, M. D., Revzin, A., 2009. Anal. Chem. 81, 8150–8156.